ACOUSTIC SCATTERING FROM A SLENDER OBJECT BY BOTTOM-BOUNCED BEAM IN DEEP WATER

Bo Lei[a,b], Yixin Yang[a,b], Yong Wang[a,b]

[a]Key Laboratory of Ocean Acoustics and Sensing (Northwestern Polytechnical University), Ministry of Industry and Information Technology, Xi'an, Shaanxi, 710072, China
[b]School of Marine Science and Technology, Northwestern Polytechnical University, Xi'an 710072, China

Corresponding author: Bo Lei
Email: lei.bo@nwpu.edu.cn

Abstract: *Bottom bounce propagation occurs when a sound ray strikes the bottom and is reflected back to the surface of the water, consequently involving an annulus. The work focuses on the scattering problem in this annulus by a beam that is deliberately transmitted downwards at relatively steep angles. A scattering model based on the virtual source concept, including evanescent waves, has been exploited. The scattering field from a slender spheroid located in the typical shadow zone has been computed and analysed with bottom-bounced incidence. Interesting scattering phenomena were observed. The results showed that the deep-water propagation and bottom bounce paths for the scattering waves always existed under the bottom bounce scheme, and that the specular scattering strength increases and directions differ with respect to the depression angles. On the horizontal plane, the propagation direction of specular scattered waves was close to the backward direction with increasing depression angle, which could be explained by the geometrical scattering theory. At depression angle of directional source ranging from 40°–50°, the bottom bounced scattered waves have more significant contribution at range approaching half of convergence range.*

Keywords: *acoustic scattering, bottom bounce, deep water*

1. INTRUDUCTION

Active sonar plays an important role in underwater detection. When a transmitter is deployed close to the sea surface in deep water, most of the energy propagates along the reliable acoustic path (RAP)[1] and refracts near the sea bottom, leading to the generation of a convergence zone (CZ). Limited acoustic energy could reach the zone between the transmitter and the first CZ. Hence, active detection in this range is problematic.

The bottom bounce propagation path in deep water has been an attractive research subject for several decades[2,3]. This scheme may provide passive detection and localization solutions. According to the reciprocity principle,[4] if a transmitted signal from an active source could propagate along the bottom bounce path, then it can arrive at the shadow zone and may touch the submerged object in this area. On the basis of this concept, simulations have been performed by deliberately directing an acoustic beam downward at relatively steep angles. A range annulus exists with CZs but without focusing gain. Although "the more incidence, the more scattering strength" is a generally accepted idea, the behavior of object scattering in this annulus is not well understood in active detection.

The current study aims to investigate the behavior of object scattering with bottom-bounced beam illumination. A slender object was located in the acoustic shadow zone of deep water. An acoustic beam with a depression angle was generated to simulate the beam reflection on the sea bottom and its propagation in the deep water. The scattering strength distributions were calculated with the virtual source concept, with the evanescent wave included inherently. Interesting scattering phenomena were observed, and physical interpretations were derived. The results showed that scattered field strength can be enhanced with a beam depression angle ranging from 40° to 50°.

2. DEEP ANGLE BEEM

According to Snell's Law, the sound in deep water is reflected on the seafloor given that the transmitted angle is deeper than the critical angle

$$\theta_{ca} = \arccos(c_0/c_b), \tag{1}$$

where c_0 and c_b are the speeds of sound at the depth of the source and the seafloor, respectively. Otherwise, the sound propagates along the RAP. In the case $c_0 > c_b$, no critical depth is present, and all the transmitted waves are reflected on the seafloor.

In this study, a directional source is utilized; thus, the pressure angular spectrum is represented by the source beam pattern. Once the angle that corresponds to the peak of the pressure angular spectrum is larger than the critical angle, most of the radiated waves travel downward and bounce on the sea bottom. This approach could be practically applied by controlling the direction of the beam. The bottom bounce configuration for active detection is exploited. Under such configuration, a directional source is manipulated such that the acoustic beam could bounce on the sea bottom and penetrate into the shadow zone. If the depression angle is properly selected, then the reflected beam can interact with the submerged object, thus enhancing the scattered echo strength.

3. OBJECT SCATTERING

3.1. Acoustical environment

In this study, a typical deep-water environment with a depth of 5000 m was considered. The Munk sound speed profile is considered. The sea bottom is covered with a 300 m-thick sediment layer with compressional wave attenuation of 0.06 dB/λ. Here, the sound speed and density are 1521 m/s and 1240 kg/m3, respectively, at the upper interface measured by Hamilton,[5] and 1622 m/s and 1650 kg/m3, respectively, at the lower interface. The gradient of the sound speed is 0.337 s^{-1}. The bottom is assumed as a half space from a depth of 5300 m with a sound speed of 1622 m/s, density of 1800 kg/m3, and compressional wave attenuation of 0.2 dB/λ. The source is located at a depth of 100 m. A 21-element vertical source array with Gaussian weights was utilized for directional source simulations. The center frequency was 500 Hz, and the adjacent element space was 1.5 m, which was approximately half of the wavelength. The source strength was set to 0 dB re 1μPa @1 m. The horizontally transmitted ray was refracted upward at a depth of 3600 m, and the maximum angle along the RAP, i.e., the critical angle, was approximately 10° according to Eq. (1). Under this acoustical environment, the pressure angular spectrum was maximized at −10° to 10° (the minus sign indicates that the rays propagated upward). If the mainlobe direction of a source exceeds the critical angle, then the transmitted waves from the mainlobe may continue to go downward until they reach the seafloor.

3.2. Scattering field from slender object

A rigid slender spheroid with a 60 m long axis and an 8 m short axis located at a depth of 180 m was considered as a scatterer. The source beam direction was horizontal (0° depression angle) and located at distances of 60 and 22 km from the object. Thus, the object was located in the first CZ and shadow zone, respectively. The directional source was at a 45° aspect angle of the slender spheroid. The scattering model named virtual source[6] combined with wavenumber integral model[7] is utilized. The scattered field is shown in Fig. 1. The scattered field was significantly stronger in the upper panel than in the lower panel because of the strong incident field in the first CZ. Similar structures on the vertical plane were also found in the forward and backward scattering fields. The deep-water propagation path and the bottom bounce path were the two main apparent propagation paths. The bottom-bounced scattered waves were transmitted within 25 km underneath the sea surface. These bottom-bounced waves showed potential applicability to active detection. However, the scattered field in the lower panel seemed to be weak when the object was submerged in the shadow zone, particularly for the backward scattered field. This phenomenon presented a challenge for active detection in the shadow zone.

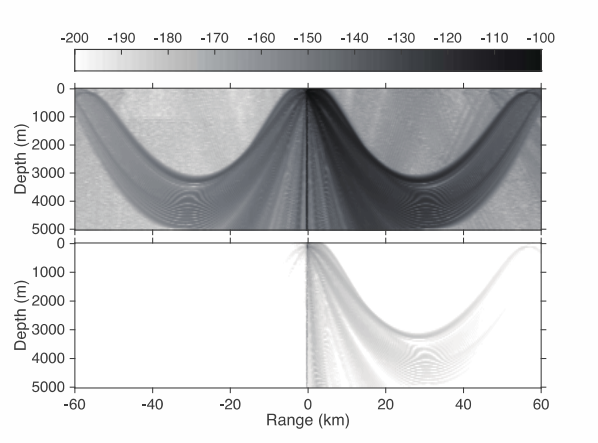

Fig 1: Scattering from a submerged object in deep water with a horizontally transmitted beam.

Given that an acoustic wave can penetrate into the shadow zone through the bottom bounce path, the scattered field at the transmitted depression ranging from 0° to 50° was considered. Some results for the scattered field are presented in Fig. 2. Under the bottom bounce configuration, the vertical scattered field in the forward and backward directions shown in Fig. 2(a) is more enhanced in comparison with that shown in the lower panel of Fig. 2. The horizontal scattered field in Fig. 2(b) indicates the existence of four lobes in the scattering pattern, which corresponded to forward scattering, backward scattering, and specular scatterings from two aspects of the object. The results with the depression angle ranging from 20° to 40° in panels (b)–(c) show the strengthening of the scattered field with increasing depression angle. Another distinguishable difference was that the forward and specular lobes deviated from 0° (solid arrow direction) and 270° (dotted arrow direction) on the horizontal plane as the depression angle increased. Such deviation can be explained from the geometrical point of view. The heading angle of the slender spheroid was represented as φ, the incident grazing angle was represented as θ, and the local incident angle β on the object with respect to the long axis can be expressed as

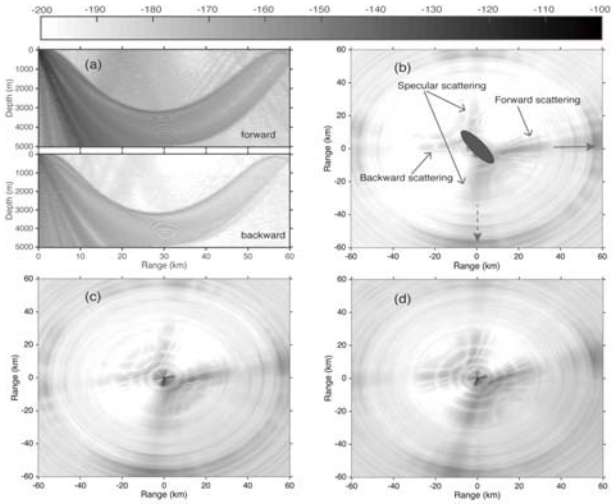

Fig 2: Scattered field strength with different depression angles. The object is located at a depth of 180 m and is close to the center of the reflected beam center.

$$\beta = \arccos \frac{1}{\sqrt{1+\tan^2\theta}\sqrt{1+\tan^2\varphi}}. \quad (2)$$

The increase in the transmitted angle led to the incidence of waves toward the lower part of the object, as well to the increase in the local incident angle β. As a consequence, the specular direction was close to the normal direction of the body, and the scattered field strength increased. As shown in panel (d), when the depression angle was 40°, the local incident angle was 57°. Thus, the specular angle of 12° deviated from the 270° direction.

3.3. Depression angle effects

The depression angle ranging from 0° to 50° on the scattered field was analysed. In the simulations, 11 receivers were deployed at depth from 100 m to 200 m with equal space. The average values on 11 elements were used to smooth the spatial variations of the field.

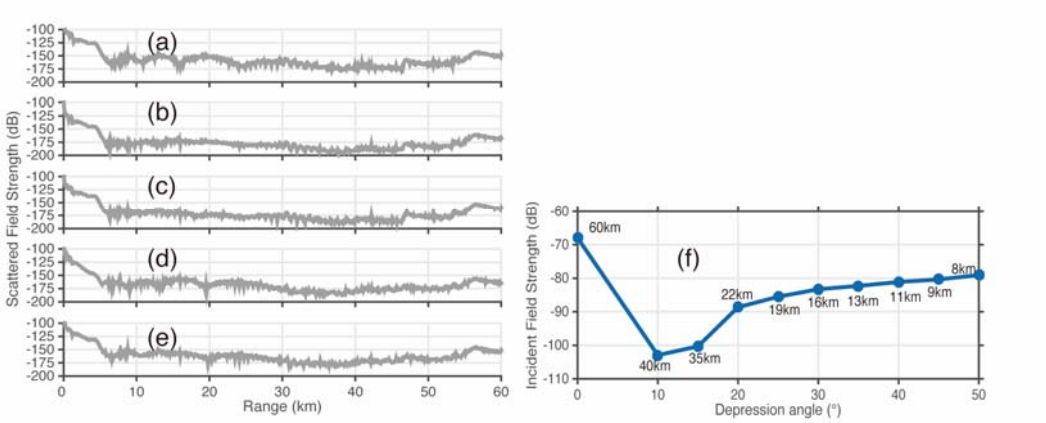

Fig 3: Average transmission loss of scattered waves on the receivers

The transmission loss of the specular scattered signal strength is plotted in Figs. 3(a)–(e). The panels from the top to the bottom have depression angles of 0°, 20°, 30°, 40°, and 50° with the object located at a depth of 180 m and at distances of 60, 22, 16, 11, and 8 km from the source (almost in the center of the first annulus), respectively. When the beam was transmitted along the horizontal direction, the scattered field strength had a relatively large value because the object was in the first CZ. Some of the scattered waves were reflected from the sea bottom, thus enhancing the field strength at approximately 8.8, 13.2, 19.5, and 30.5 km. When the beam was transmitted 20° downward to the sea bottom, the strength decreased (Fig. 3(b)) because of the reduced incident field strength. As discussed previously, a portion of the transmitted waves propagated along the RAP because their transmitted angles in the mainlobe were smaller than the critical angle. However, when the depression angle continued to increase above 30°, the strength was enhanced within the first CZ range, as indicated in panels (c) to (e). One reason for this enhancement was the slight strengthening of the incident field in the shadow zone as a result of the large depression angle, as presented in Fig. 3(f). Another reason was that at large depression angles, the waves were incident toward the lower parts of the object; they then scattered and propagated downward until they reached the sea bottom. As a result, the scattered field strength was elevated. That's to say, in cases in which the beam was transmitted downward, an optimum field strength enhancement was achieved with a 40°−50° depression angle in the range not exceeding the first CZ.

4. CONCLUSIONS

Some simplifications were made, and scattering from the submerged slender spheroid was analysed when it was located in the shadow zone. On the horizontal plane, the propagation direction of the specular scattered waves was close to the backward direction as the depression angle increased. The scattered field showed a deep-water propagation path convergence at approximately 55 km. In a range not exceeding 25 km, the scattered field increased because of the contribution from the bottom-reflected propagation path. With a 40°–50° depression angle, the scattered field within the first CZ range showed an apparent enhancement relative to that in other angles.

5. ACKNOWLEDGEMENTS

This work was supported by the National Natural Science Foundation of China (61571366) and the National Key Technologies R&D Program (2016YFC1400200).

REFERENCES

[1] R. J. Urick, *Principles of underwater sound*. New York: McGraw-Hill Book Company, 1983.

[2] A. Winder, "II. Sonar system technology," *Sonics Ultrason. IEEE Trans.*, vol. 22, no. 5, pp. 291–332, 1975.

[3] W. M. X. Zimmer, M. P. Johnson, A. D'Amico, and P. L. Tyack, "Combining data from a multisensor tag and passive sonar to determine the diving behavior of a sperm whale (physeter macrocephalus)," *IEEE J. Ocean. Eng.*, vol. 28, no. 1, pp. 13–28, 2003.

[4] F. B. Jensen, W. A. Kuperman, M. B. Porter, and H. Schmidt, *Computational ocean acoustics*. Springer Science & Business Media, 2011.

[5] E. Hamilton, "Sound velocity and related properties of marine sediments, North Pacific," *J. Geophys. Res.*, vol. 75, no. 23, pp. 4423–4446, 1970.

[6] H. Schmidt, "Virtual source approach to scattering from partially buried elastic targets," *High Freq. Ocean Acoust.*, vol. 728, pp. 456–463, 2004.

[7] H. Schmidt and J. Glattetre, "A fast field model for three-dimensional wave propagation in stratified environments based on the global matrix method," *J. Acoust. Soc. Am.*, vol. 78, no. 6, pp. 2105–2114, 1985.